

High-Mobility Tri-Gate β -Ga₂O₃ MESFETs with a Power Figure of Merit over 0.9 GW/cm²

Arkka Bhattacharyya, Saurav Roy, Praneeth Ranga, Carl Peterson, and Sriram Krishnamoorthy

Abstract— In this letter, fin-shape tri-gate β -Ga₂O₃ lateral MESFETs are demonstrated with a high power figure of merit (PFOM) of 0.95 GW/cm² – a record high for any β -Ga₂O₃ transistor to date. A low-temperature undoped buffer-channel stack design is developed which demonstrates record high Hall and drift electron mobilities in doped β -Ga₂O₃ channels allowing for low ON resistances (R_{ON}) in β -Ga₂O₃ MESFETs. Fin-widths (W_{fin}) were 1.2-1.5 μ m and there were 25 fins (N_{fin}) per device with a trench depth of $\sim 1 \mu$ m. A β -Ga₂O₃ MESFET with a source-drain length of 6.4 μ m exhibits a high ON current (187 mA/mm), low R_{ON} (20.5 Ω .mm) and a high average breakdown field (4.2 MV/cm). All devices show very low reverse leakage until catastrophic breakdown for breakdown voltages (V_{BR}) scaled from 1.1kV to ~ 3 kV. This work demonstrates the potential of channel engineering in improving β -Ga₂O₃ device performance toward lower conduction losses for low-to-medium voltage applications.

Index Terms— Ga₂O₃, power device, MESFETs, finFETs, MOVPE, regrown contacts, breakdown, kilovolt, power figure of merit, passivation.

I. INTRODUCTION

Ultra-wide bandgap (UWBG) β -Ga₂O₃ ($E_g = 4.6 - 4.9$ eV) material and device technology is maturing rapidly and offers enormous opportunities for next-generation solid-state power switching with improved system-level size, weight, and power (SWaP) efficiency. β -Ga₂O₃ is the only UWBG semiconductor that offers the advantage of producing large area native bulk substrates from melt-grown techniques – offering potentially lowered costs for large-scale manufacturing at a much higher device yield and uniformity[1],[2]. Thanks to its compatibility with the established WBG process technology and single crystal growth using standard epitaxial techniques, β -Ga₂O₃ material and device performance has improved rapidly with lateral and vertical β -Ga₂O₃ devices demonstrating class-leading blocking voltages (up to 8kV) and breakdown field strengths (>5 MV/cm)[3]–[10].

Although β -Ga₂O₃ devices have demonstrated tremendous performance advantages, its performance is still far from its projected intrinsic material limit. β -Ga₂O₃ transistors with high breakdown voltages and PFOMs have been realized which

have focused mainly on electric field management techniques for improving average breakdown fields and device scaling for improving ON resistances[3], [5], [11]–[13]. However, less attention has been paid to doped channel design and engineering for improving electron mobility toward lowered device ON resistance[14]–[16]. In this letter, we demonstrate an improved channel stack design with low-temperature metalorganic vapor phase epitaxy (MOVPE) grown un-doped buffer layers with record high Hall and drift electron mobilities in doped β -Ga₂O₃ channels. By fabricating fin-shape tri-gate β -Ga₂O₃ MESFETs, PFOM close to 1 GW/cm² and multi-kV breakdown voltages (over 2kV) are achieved simultaneously.

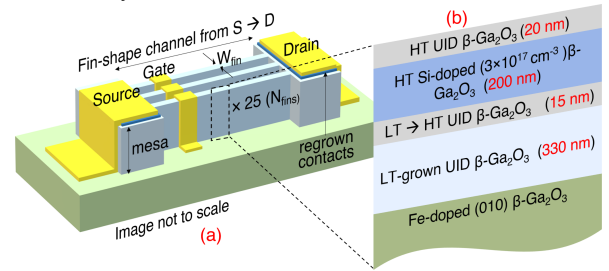


Fig. 1. (a) 3D schematic of the tri-gate β -Ga₂O₃ MESFETs (with a SiN_x wrap-around passivation not shown). (b) 2D cross-section schematic of the channel stack.

II. DEVICE GROWTH AND FABRICATION

For the channel design, a hybrid low temperature - high temperature (LT-HT) undoped buffer/doped channel epitaxial stack is grown using MOVPE. The (010) Fe-doped Ga₂O₃ substrates (NCT, Japan) were cleaned in HF (49%) for 30 mins prior to channel growth [17]. The epitaxial structure was grown using an Agnitron Agilis MOVPE reactor with TEGa, O₂ and silane (SiH₄) as precursors and argon as carrier gas. An LT (600°C) undoped Ga₂O₃ buffer (330 nm thick) is grown followed by transition layers to a HT (810°C) Si-doped Ga₂O₃ channel layers (~ 200 nm) without growth interruption[18].

Fin-shape MESFETs were fabricated with a channel stack whose Hall mobility, sheet charge (electron density) and R_{sh} were 168 cm²/Vs, 5.8×10^{12} cm⁻² ($\sim 3 \times 10^{17}$ cm⁻³), and 6.4 k Ω/\square , respectively. The channel stack cross-section schematic is shown in Figure 1(b). Fin-shape channels with length (L_{fin}) that run from the source to the drain ($L_{fin} \sim L_{SD}$) were formed using Ni/SiO₂ mask pattern and SF₆-Ar ICP-RIE dry etch with trench depths $\sim 1 \mu$ m (3D schematic shown in Figure 1(a)) [19]. After the dry etching step, wet acid treatments using room temperature diluted HCl (20 mins) and diluted HF (10 mins) were used for dry-etch-induced surface damage recovery. Planar LT-MOVPE regrown ohmic contacts were employed [12]. The estimated electron concentration in the regrown contact layer is around $n \sim 1.4 \times 10^{20}$ cm⁻³. Ti/Au/Ni (20/150/50 nm) ohmic metal was evaporated on the regrown contacts and annealed at 450°C for 1.5 mins in N₂ ambient[12]. Ni/Au/Ni (30/100/30 nm) gates were evaporated

This material is based upon work supported by the II-VI foundation Block Gift Program 2020-2022. This material is also based upon work supported by the Air Force Office of Scientific Research under award number FA9550-21-0078 (Program Manager: Dr. Ali Sayir).

A. Bhattacharyya & P. Ranga are with the Department of Electrical and Computer Engineering, University of Utah, Salt Lake City, Utah, USA 84112.

S. Roy, C. Peterson and S. Krishnamoorthy are with Materials Department, University of California, Santa Barbara, California, USA 93106. (email: sriramkrishnamoorthy@ucsb.edu).

*corresponding author email: a.bhattacharyya@utah.edu.

to form the Schottky gates. The whole device was passivated using a ~ 250 nm PECVD (300°C) deposited SiN_x dielectric. Lateral device dimensions were verified by SEM. Fin-widths (W_{fin}) were 1.2-1.5 μm , trench widths were ~ 5.3 μm and there were 25 fins (N_{fin}) per device. The L_{GS} and L_{G} were fixed at 2.4 μm and 1.3 μm and the L_{GD} was varied from 2.7 to 16.7 μm on the same wafer. Concentric Schottky gate CV pads (220 μm diameter) and fatFETs structures were also fabricated on the same MESFET sample.

III. RESULTS AND DISCUSSIONS

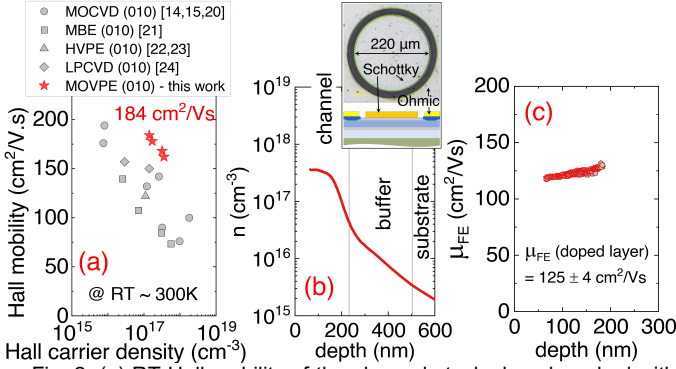


Fig. 2. (a) RT Hall mobility of the channel stacks benchmarked with various state-of-the-art reports [14], [15], [20]–[24]. (b) & (c) channel charge profile extracted from C-V measurements (inset: CV pad image and cross-section schematic) and RT field-effect mobility depth profile in the doped β -Ga₂O₃ MESFET channel, respectively.

From room temperature (RT) Hall measurements, this stack design is shown to have an effective RT Hall mobility value in the range 162 – 184 cm²/Vs for doped channel electron densities of $1.5 - 3.5 \times 10^{17}$ cm⁻³ measured on multiple samples/substrates. It is hypothesized that the enhanced channel mobility could be due to lower Fe riding into the channel from the substrate due to the lower growth temperature of the buffer as well as the absence of any low-mobility parasitic channel near the substrate [25], [26]. Further details and characterization of this stack design will be reported elsewhere. These Hall mobility values are record high for any doped Ga₂O₃ channel to date as it is compared with the state-of-the-art values reported utilizing various growth techniques in Figure 2(a).

Charge profile of the MESFET channel extracted from capacitance-voltage measurement is shown in Figure 2(b). It shows that the buffer is completely depleted and there is no active parasitic channel at the epilayer-substrate interface. These further supports ascribing the measured Hall and drift mobility to only the doped channel layer. The channel mobility of the MESFET was characterized using fatFET devices ($L_{\text{G}} \sim 103$ μm , $L_{\text{GS}}/L_{\text{GD}} \sim 1$ μm) in the linear region of the device operation. Under a low drain bias ($V_{\text{DS}} = 0.1$ V), the field-effect mobility μ_{FE} can be related to the transconductance as, $\mu_{\text{FE}} = (g_{\text{m}} \times L_{\text{G}}^2) / (C_{\text{G}} \times V_{\text{DS}})$ where g_{m} , L_{G} , C_{G} , V_{DS} are the transconductance, gate length, gate-to-channel capacitance and applied drain bias respectively. Figure 2(c) shows the room-temperature depth profile of the extracted μ_{FE} in the doped channel. The μ_{FE} showed an average value of ~ 125 cm²/Vs with a peak value of 132 cm²/Vs which is the highest electron drift mobility value ever reported in a uniformly doped β -Ga₂O₃ channels.

Figure 3(a) and 3(b) shows the DC output and transfer curves for the fin-shape MESFET with dimensions $L_{\text{GS}}/L_{\text{G}}/L_{\text{GD}} = 2.4/1.3/2.7$ μm . The ON current and resistance were normalized to the device width ($W_{\text{fin}} \times N_{\text{fin}}$). The devices show clear current saturation and low saturation voltages ($V_{\text{DS,Sat}}$). The maximum ON current measured was 187 mA/mm. The ON resistance (R_{ON}) extracted from the linear region of the output curves were found to be 20.5 $\Omega\cdot\text{mm}$. From TLM measurements, the total R_{C} (contact resistance) to the channel was extracted to be 1.0 ± 0.2 $\Omega\cdot\text{mm}$ ($\leq 5\%$ of the total device R_{ON}). The devices show sharp pinch off with low sub threshold swing (156 mV/dec) and threshold voltage of -10 V. From the transfer curves, the devices show low leakage ($\sim 10^{-11}$ A/mm) and high $I_{\text{ON}}/I_{\text{OFF}}$ ratio $\sim 10^{10}$. The transistors also exhibit very low gate leakage and high transconductance peak of 12.6 mS/mm. The hysteresis effects seem to be minimal as shown in Figure 3(c) and 3(d) dual sweep I-V curves. These devices exhibit a negligible hysteresis of $\Delta V \sim 0.06$ V. Dynamic performance characterization is required in the future to ascertain any deleterious effect of low temperature buffers and any resultant charge trapping.

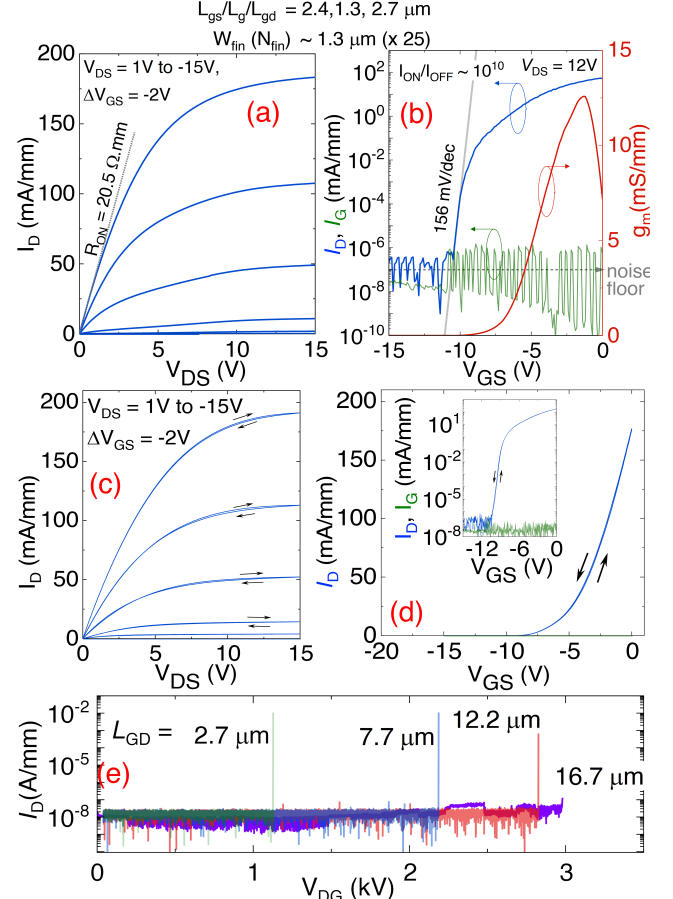


Fig.3. DC (a) output and (b) transfer curves of the tri-gate β -Ga₂O₃ MESFETs. Dual sweep linear DC (c) output and (d) transfer I-V hysteresis curves (inset: semilog plot) of a device with the same dimensions. (e) Off-state breakdown characteristics of the tri-gate β -Ga₂O₃ MESFETs with various L_{GD} values.

Figure 3(e) shows the three-terminal breakdown characteristics (at $V_{\text{GS}} = -35$ V) of the MESFETs with various L_{GD} values. All the breakdown measurements were performed with the wafer submerged in FC-40 Fluorinert dielectric liquid. The device breakdown was catastrophic (destructive)

with negligible reverse leakage until the breakdown occurred. The reverse leakage during the breakdown measurements were limited by the measurement tool (Keysight B1505 with 3kV HV SMU). It is seen in Figure 3(c) that the V_{BR} ($= V_{DS}-V_{GS}$) scaled from 1.1kV to ~ 3 kV as the L_{GD} was scaled from 2.7 to 16.7 μ m.

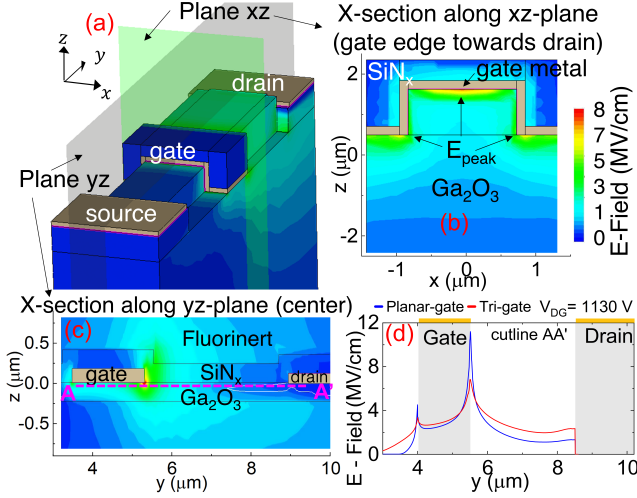


Fig.4 (a) Simulated 3D (SiN_x & Fluorinert partly hidden for visibility) (b)&(c) X-section E-field contours along two planes of the tri-gate design with $L_{GD} = 3\mu\text{m}$, and $V_{DG} = 1130\text{V}$. (d) E-field profile of the same FET (cutline AA' under the gate) comparing planar-gate and tri-gate.

From the cross-section (xz-plane Figure 1(a,b)) of the 3D TCAD simulated structure (with $L_{GD} = 3\mu\text{m}$, and $V_{DG} = 1130\text{V}$) at the gate edge towards drain, it is shown that the peak fields are at the center of the top gate and gate metal corners in the etched region. Hence, in the presence of the UID cap layer and deeper trenches, peak fields are present in the UID cap region and the insulating substrate. When this design is compared with a planar gate structure (Figure 4(d)), the tri-gate exhibits lower peak field at the gate edge (without the need for field plates), improving the E_{AVG} values in the drift region dramatically.

Figure 5(a) shows the variation of V_{BR} and the effective average field ($E_{AVG} = V_{BR}/L_{GD}$) as a function of L_{GD} . The maximum E_{AVG} achieved was ~ 4.2 MV/cm for the smallest device with L_{GD} of 2.7 μm ($V_{BR} = 1.13$ kV). This is the highest reported average breakdown field for $L_{GD} > 1\mu\text{m}$ [3], [27]. The E_{AVG} decreased monotonously as the V_{BR} increased with increasing L_{GD} . For a V_{BR} of ~ 3 kV and L_{GD} of 16.7 μm , the E_{AVG} is 1.8 MV/cm. Since this is the first report of LT MOVPE-grown buffers in β -Ga₂O₃ devices, further study combining field plates and buffer breakdown structures will be necessary to elucidate on factors limiting the breakdown performance in these devices, especially at higher L_{GD} . Nevertheless, the high ON currents (low R_{ON}), the high V_{BR} , E_{AVG} and low reverse leakage behavior simultaneously demonstrated in these first-generation LT-buffer devices are a significant improvement over the state-of-the-art β -Ga₂O₃-based transistors.

Since these devices utilized fin lengths running from source to drain, an effective channel area of $(L_{SD} + 2L_T) \times W_{fin} \times N_{fin}$ was used to normalize the ON resistance. L_T , the transfer length, is extracted from TLM structures to be 0.2 μm . The PFOM values for fin-shape MESFETs are plotted as a function of L_{GD} (Fig.5(b)). The highest PFOM of 0.95 GW/cm² was calculated for MESFETs with L_{GD} of 2.8 μm and

7.7 μm which had V_{BR} of 1.1 kV and 2.2 kV, respectively. The PFOM of the devices with L_{GD} of 12.2 μm and 16.7 μm were 0.65 GW/cm² ($V_{BR} = 2.8\text{kV}$) and 0.44 GW/cm² ($V_{BR} \sim 3$ kV). The PFOM of the large L_{GD} devices were a bit lower due to lower E_{AVG} values compared to the small L_{GD} devices, as discussed earlier. Nevertheless, the PFOM reported for > 2 kV devices are still the highest reported values. Figure 5(c) benchmarks the PFOM values of the fin-shape MESFETs with the existing literature reports. It is compared with state-of-the-art β -Ga₂O₃-based transistors that include advanced designs like Ga₂O₃ MOSFETs, (AlGa)₂O₃/Ga₂O₃ HFETs and p-n hetero-junction β -Ga₂O₃ FETs. It shows the reported PFOM of 0.95 GW/cm² is a record high for any β -Ga₂O₃ transistor to date. Further improvement can be expected by implementing E-field management techniques like field-plates, planar access regions, gate dielectrics with high breakdown field strengths, higher channel charge, higher channel mobility and lowering reverse leakage simultaneously.

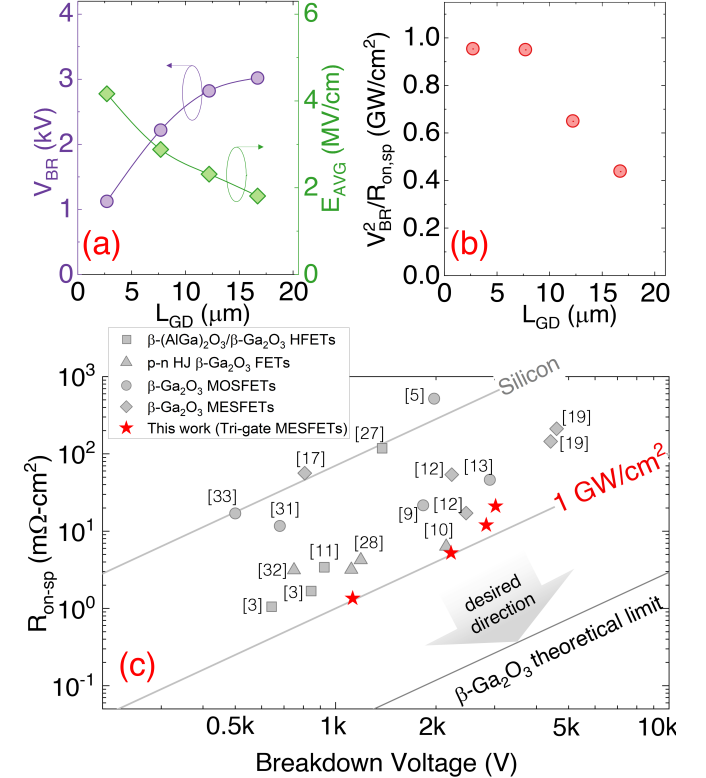


Fig.5 (a) V_{BR} and E_{AVG} , (b) PFOM as a function of L_{GD} . (c) Differential $R_{on,sp}-V_{BR}$ benchmark plot of our Tri-gate β -Ga₂O₃ MESFETs with the literature reports [3], [4], [4], [5], [9]–[11], [13], [28]–[33].

IV. CONCLUSION

We demonstrate over 0.9 GW/cm² PFOM in multi-kV fin-shape β -Ga₂O₃ lateral MESFETs – a record high for any β -Ga₂O₃ transistor to date. An LT-HT buffer-channel stack is demonstrated using MOVPE with record high RT Hall and drift mobilities in doped β -Ga₂O₃ channels. Using tri-gates, β -Ga₂O₃ MESFETs with high ON currents, negligible hysteresis effects and low ON resistances are realized with very low reverse leakage and V_{BR} values of 1.1kV to ~ 3 kV. These devices show great potential of high-performance β -Ga₂O₃ FETs for future power device applications in the low to medium voltage range.

V. REFERENCES

- [1] M. Higashiwaki and G. H. Jessen, "Guest editorial: The dawn of gallium oxide microelectronics," *Appl. Phys. Lett.*, vol. 112, no. 6, Feb. 2018, Art. no. 060401, doi: 10.1063/1.5017845.
- [2] S. J. Pearton, J. Yang, P. H. Cary, F. Ren, J. Kim, M. J. Tadjer, and M. A. Mastro, "A review of Ga₂O₃ materials, processing, and devices," *Appl. Phys. Rev.*, vol. 5, no. 1, Mar. 2018, Art. no. 011301, doi: 10.1063/1.5006941.
- [3] N. K. Kalarickal *et al.*, " β -(Al_{0.18}Ga_{0.82})₂O₃/Ga₂O₃ double heterojunction transistor with average field of 5.5 MV/cm," *IEEE Electron Device Lett.*, vol. 42, no. 6, pp. 899–902, Jun. 2021, doi: 10.1109/LED.2021.3072052.
- [4] A. J. Green *et al.*, "3.8-MV/cm breakdown strength of MOVPE-grown Sn-doped β -Ga₂O₃ MOSFETs," *IEEE Electron Device Lett.*, vol. 37, no. 7, pp. 902–905, Jul. 2016, doi: 10.1109/LED.2016.2568139.
- [5] S. Sharma, K. Zeng, S. Saha, and U. Singiseti, "Field-Plated Lateral Ga₂O₃ MOSFETs With Polymer Passivation and 8.03 kV Breakdown Voltage," *IEEE Electron Device Letters*, vol. 41, no. 6, pp. 836–839, Jun. 2020, doi: 10.1109/LED.2020.2991146.
- [6] S. Roy, A. Bhattacharyya, P. Ranga, H. Splawn, J. Leach, and S. Krishnamoorthy, "High-k Oxide Field-Plated Vertical (001) β -Ga₂O₃ Schottky Barrier Diode With Baliga's Figure of Merit Over 1 GW/cm²," *IEEE Electron Device Letters*, vol. 42, no. 8, pp. 1140–1143, Aug. 2021, doi: 10.1109/LED.2021.3089945.
- [7] Z. Xia *et al.*, "Metal/BaTiO₃/ β -Ga₂O₃ dielectric heterojunction diode with 5.7 MV/cm breakdown field," *Appl. Phys. Lett.* 115, 252104 (2019).
- [8] P. Dong *et al.*, "6 kV/3.4 mΩ·cm² Vertical β -Ga₂O₃ Schottky Barrier Diode With BV²/R_{on,sp} Performance Exceeding 1-D Unipolar Limit of GaN and SiC," *IEEE Electron Device Letters*, vol. 43, no. 5, pp. 765–768, May 2022, doi: 10.1109/LED.2022.3160366.
- [9] K. Tetzner *et al.*, "Lateral 1.8 kV β -Ga₂O₃ MOSFET With 155 MW/cm² Power Figure of Merit," *IEEE Electron Device Letters*, vol. 40, no. 9, pp. 1503–1506, Sep. 2019, doi: 10.1109/LED.2019.2930189.
- [10] C. Wang *et al.*, "Hysteresis-free and μ s-switching of D/E-modes Ga₂O₃ hetero-junction FETs with the BV²/R_{on,sp} of 0.74/0.28 GW/cm²," *Appl. Phys. Lett.*, vol. 120, no. 11, p. 112101, Mar. 2022, doi: 10.1063/5.0084804.
- [11] N. K. Kalarickal *et al.*, "Electrostatic Engineering Using Extreme Permittivity Materials for Ultra-Wide Bandgap Semiconductor Transistors," *IEEE Transactions on Electron Devices*, vol. 68, no. 1, pp. 29–35, Jan. 2021, doi: 10.1109/TED.2020.3037271.
- [12] A. Bhattacharyya *et al.*, "Multi-kV Class β -Ga₂O₃ MESFETs With a Lateral Figure of Merit Up to 355 MW/cm²," *IEEE Electron Device Letters*, vol. 42, no. 9, pp. 1272–1275, 2021, doi: 10.1109/LED.2021.3100802.
- [13] Y. Lv *et al.*, "Lateral β -Ga₂O₃ MOSFETs With High Power Figure of Merit of 277 MW/cm²," *IEEE Electron Device Letters*, vol. 41, no. 4, pp. 537–540, Apr. 2020, doi: 10.1109/LED.2020.2974515.
- [14] Z. Feng, A. F. M. Anhar Uddin Bhuiyan, M. R. Karim, and H. Zhao, "MOCVD homoepitaxy of Si-doped (010) β -Ga₂O₃ thin films with superior transport properties," *Appl. Phys. Lett.*, vol. 114, no. 25, p. 250601, Jun. 2019, doi: 10.1063/1.5109678.
- [15] Z. Feng *et al.*, "Probing Charge Transport and Background Doping in Metal-Organic Chemical Vapor Deposition-Grown (010) β -Ga₂O₃," *physica status solidi (RRL) – Rapid Research Letters*, vol. 14, no. 8, p. 2000145, 2020, doi: <https://doi.org/10.1002/pssr.202000145>.
- [16] G. Seryogin *et al.*, "MOCVD growth of high purity Ga₂O₃ epitaxial films using trimethylgallium precursor," *Appl. Phys. Lett.*, vol. 117, no. 26, p. 262101, Dec. 2020, doi: 10.1063/5.0031484.
- [17] A. Bhattacharyya *et al.*, "130 mA mm⁻¹ β -Ga₂O₃ metal semiconductor field effect transistor with low-temperature metalorganic vapor phase epitaxy-regrown ohmic contacts," *Appl. Phys. Express*, vol. 14, no. 7, p. 076502, Jun. 2021, doi: 10.35848/1882-0786/ac07ef.
- [18] A. Bhattacharyya, P. Ranga, S. Roy, J. Ogle, L. Whittaker-Brooks, and S. Krishnamoorthy, "Low temperature homoepitaxy of (010) β -Ga₂O₃ by metalorganic vapor phase epitaxy: Expanding the growth window," *Applied Physics Letters*, vol. 117, no. 14, p. 142102, 2020, doi: 10.1063/5.0023778.
- [19] A. Bhattacharyya *et al.*, "4.4 kV β -Ga₂O₃ MESFETs with power figure of merit exceeding 100 MW/cm²," *Appl. Phys. Express*, vol. 15, no. 6, p. 061001, May 2022, doi: 10.35848/1882-0786/ac6729.
- [20] Y. Zhang *et al.*, "MOCVD grown epitaxial β -Ga₂O₃ thin film with an electron mobility of 176 cm²/V s at room temperature," *APL Materials*, vol. 7, no. 2, p. 022506, Dec. 2018, doi: 10.1063/1.5058059.
- [21] K. Sasaki, A. Kuramata, T. Masui, E. G. Villora, K. Shimamura, and S. Yamakoshi, "Device-Quality β -Ga₂O₃ Epitaxial Films Fabricated by Ozone Molecular Beam Epitaxy," *Appl. Phys. Express*, vol. 5, no. 3, p. 035502, Feb. 2012, doi: 10.1143/APEX.5.035502.
- [22] J. H. Leach, K. Udway, J. Rumsey, G. Dodson, H. Splawn, and K. R. Evans, "Halide vapor phase epitaxial growth of β -Ga₂O₃ and α -Ga₂O₃ films," *APL Materials*, vol. 7, no. 2, p. 022504, Feb. 2019, doi: 10.1063/1.5055680.
- [23] H. Murakami *et al.*, "Homoepitaxial growth of β -Ga₂O₃ layers by halide vapor phase epitaxy," *Appl. Phys. Express*, vol. 8, no. 1, p. 015503, Dec. 2014, doi: 10.7567/APEX.8.015503.
- [24] Y. Zhang, Z. Feng, M. R. Karim, and H. Zhao, "High-temperature low-pressure chemical vapor deposition of β -Ga₂O₃," *Journal of Vacuum Science & Technology A*, vol. 38, no. 5, p. 050806, Sep. 2020, doi: 10.1116/6.0000360.
- [25] A. Mauze *et al.*, "Investigation of unintentional Fe incorporation in (010) β -Ga₂O₃ films grown by plasma-assisted molecular beam epitaxy," *Appl. Phys. Lett.* 115, 052102 (2019).
- [26] C. Joishi *et al.*, "Effect of buffer iron doping on delta-doped β -Ga₂O₃ metal semiconductor field effect transistors," *Appl. Phys. Lett.*, vol. 113, no. 12, p. 123501, Sep. 2018, doi: 10.1063/1.5039502.
- [27] C. Joishi *et al.*, "Breakdown Characteristics of β - (Al_{0.22}Ga_{0.78})₂O₃/Ga₂O₃ Field-Plated Modulation-Doped Field-Effect Transistors," *IEEE Electron Device Letters*, vol. 40, no. 8, pp. 1241–1244, Aug. 2019, doi: 10.1109/LED.2019.2921116.
- [28] C. Wang *et al.*, "Demonstration of the p-NiOx/n-Ga₂O₃ Heterojunction Gate FETs and Diodes With BV²/R_{on,sp} Figures of Merit of 0.39 GW/cm² and 1.38 GW/cm²," *IEEE Electron Device Letters*, vol. 42, no. 4, pp. 485–488, Apr. 2021, doi: 10.1109/LED.2021.3062851.
- [29] K. Zeng, A. Vaidya, and U. Singiseti, "1.85 kV Breakdown Voltage in Lateral Field-Plated Ga₂O₃ MOSFETs," *IEEE Electron Device Letters*, vol. 39, no. 9, pp. 1385–1388, Sep. 2018, doi: 10.1109/LED.2018.2859049.
- [30] K. Zeng, A. Vaidya, and U. Singiseti, "A field-plated Ga₂O₃ MOSFET with near 2-kV breakdown voltage and 520 mS/Ω," *Appl. Phys. Express*, vol. 12, no. 8, p. 081003, Jul. 2019, doi: 10.7567/1882-0786/ab2e86.
- [31] Y. Lv *et al.*, "Source-Field-Plated β -Ga₂O₃ MOSFET With Record Power Figure of Merit of 50.4 MW/cm²," *IEEE Electron Device Letters*, vol. 40, no. 1, pp. 83–86, Jan. 2019, doi: 10.1109/LED.2018.2881274.
- [32] K. Tetzner *et al.*, "SnO/ β -Ga₂O₃ heterojunction field-effect transistors and vertical p-n diodes," *Appl. Phys. Lett.* 120, 112110 (2022).
- [33] K. D. Chabak *et al.*, "Recessed-Gate Enhancement-Mode β -Ga₂O₃ MOSFETs," *IEEE Electron Device Letters*, vol. 39, no. 1, pp. 67–70, Jan. 2018, doi: 10.1109/LED.2017.2779867.